Sound-scattering properties of Sierpinski triangle fractal structures in the near field

Lingge Tan [a], Jieun Yang [b], Jian Kang [c], Hongpeng Xu [a*]

[a] School of Architecture, Harbin Institute of Technology; Key Laboratory of Cold Region Urban and Rural Human Settlement Environment Science and Technology, Ministry of Industry and Information Technology, Harbin 150006, China

[b] Department of the Built Environment, Eindhoven University of Technology, P.O. Box 513, 5600 MB Eindhoven, Netherlands

[c] Institute for Environmental Design and Engineering, The Bartlett, University College London, London WC1H 0NN, UK

Abstract: This paper proposes a new design of an acoustic diffuser based on the construction rules of the Sierpinski triangle in order to broaden the effective diffusion frequency range. The diffuser is made of triangular blocks of different sizes attached to a plane surface. The effects of the number of fractal iterations, the height of triangular blocks, and arrangements of the blocks on the normal-incidence diffusion coefficients in the near field are examined through numerical simulations based on the boundary element method (BEM) in the frequency range of 100 Hz – 5 kHz. Furthermore, measurement results will be presented to validate the diffusion performance presented by the numerical simulations. The diffusion performance of a conventional quadratic residue diffuser (QRD) is compared to confirm the advantage of the designed diffuser for broadening the effective frequency range. It shows that the fractal patterns with various sizes of blocks improve diffusion performance compared to the conventional QRD of the same size, especially in the mid-low frequency range below 1 kHz.

Keywords: Acoustic Diffuser; Diffusion Coefficient; Fractals; Sierpinski Triangle

1. Introduction

Acoustic diffusers are structured surfaces to improve the diffuseness of the sound distribution in a room. The use of acoustic diffusers is in some cases an efficient way to achieve a desirable acoustical environment by promoting spaciousness, preventing echoes, and improving speech intelligibility in a variety of architectural spaces [1]. The diffusers can be designed in various forms, for example, collection of hemisphere and cube blocks [2,3], one- and two-dimensional grooves [4–6], curved surfaces [7,8], or any other topologies [9] and vegetations [10]. Nowadays, advanced manufacturing techniques allow the production of more complex structures, and several examples of diffusive surfaces manufactured by 3D printers, CNC milling machines, and industrial robots can be found in recent studies [11−13].

Among the design of diffusers presented so far, the Schroeder diffusers [14,15], which are periodic diffusive surfaces made of quarter-wavelength resonant wells of which depths are determined by a mathematical sequence, have been the representative design of the acoustic diffusers for decades and have been applied in various acoustical spaces. Moreover, the improvement of its performance has been a subject of many studies, including optimization of the well depths [16−19] and adoption of metamaterial design approaches [20,21]. However, the Schroeder diffuser has limitations in the diffusion performances by its design methodology. Firstly, the bandwidth of a Schroeder diffuser is governed by the maximum depth of the well. Thus, to target the low-frequency range, the thickness of the diffuser should be larger. In addition, as pointed out in Ref. [19], the periodicity of the Schroeder diffuser produces the concentration of scattered energy in certain directions. With the change of architectural tastes over centuries, the design of the Schroeder diffuser is being questioned as well: the monotonous form of the Schroeder diffuser no longer meets the aesthetic demands of modern interface design [22].

Adapting to the parametric demands of interface design, fractals are widely applied as a fusion of mathematical calculation and artistic design. It is generally accepted that theoretical fractals are infinitely self-similar, fractal dimensions are included in the mathematical constructions, and fractal models with varying self-similarity degrees can be achieved by iterations[23]. Cox [24] presented fractal theory into the Schroeder diffuser to make a fractal vertical shape to extend the bandwidth of the quadratic residue diffusers (QRDs). Lee et al.[25] showed that organizing modules in a fractal manner can improve the diffusion capacity of diffusers across a broad frequency range through a scale model experiment. Bradley et al. [26,27] proposed the virtual 1-D fractal surfaces generated using the Random Midpoint Displacement (RMD), the acoustic effect of fractal design parameters has been presented using the numerical predictions and experimental measurement. Perry et al. [28] developed a framework to optimize acoustic diffusers in a reasonable time without the need for boundary element predictions, and in the process, the modular fractal forms have been generated to extend the bandwidth.

As one of the most famous fractal patterns, the Sierpinski triangle is a self-similar structure discovered by Waclaw Sierpinski in the 1900s[29]. Xu et al.[30] investigated the visual acceptance of the Sierpinski fractal multi-level modular diffuser through eye-tracking and semantic differential technique and found a more impressing appearance than conventional QRDs. However, the acoustic diffusion performance of such Sierpinski fractal pattern has not been considered yet, which motivated this study to propose the advanced shape combined with fractal expansion to meet both acoustic and aesthetic demands. Fractal surfaces of Sierpinski-triangles bring the possibility to avoid periodic profile, which not only improves the uneven sound field but also satisfies aesthetic needs.

In this paper, a new design methodology of a modular diffuser is proposed. The methodology is based on the construction rules of the Sierpinski triangle and provides the fractal expansion to broaden the design frequency range for those types of diffusers. The diffuser is made of triangular blocks of different sizes attached to a plane surface. The effect of the number of iterations, the height of modules, and arrangements of the blocks on the normal-incidence diffusion coefficients are examined through numerical simulations based on the boundary element method (BEM). Furthermore, measurement results will be presented to validate the diffusion performance presented by the numerical calculation. The diffusion performance of a two-dimensional QRD is compared to confirm the advantage of the designed diffuser for broadening the effective frequency range. In this work, the performance of the diffusers was evaluated in near-field conditions. This choice was made in consideration of the distances of the sound source and receivers from a diffuser surface in actual rooms.

2. Design of Sierpinski-triangle diffusers

The Sierpinski triangle is a self-similar structure with the overall shape of a triangle and subdivided recursively into smaller triangles [29]. We used isosceles right triangles as the base of the fractal pattern to make the designed diffusers easily integrated into the surfaces of buildings (e.g., walls, facades). The construction steps of the Sierpinski triangle are shown in Fig. 1(a). It starts with an isosceles right triangle (iteration 0). The triangle is subdivided into four smaller right-angled triangles by connecting the midpoints of the sides of the original one and then the triangle in the center is removed (iteration 1). Subsequently, repeating the last step with the remaining three smaller triangles results in nine triangles of a smaller scale (iteration 2). If the step is repeated once more, 27 triangles can be made (iteration 3). Then, we combine two identical right-angled Sierpinski triangle units to form a rectangle, as shown in Fig. 1(b). The black and white parts in Fig. 1 become base plane surfaces and surfaces of triangular blocks, respectively.
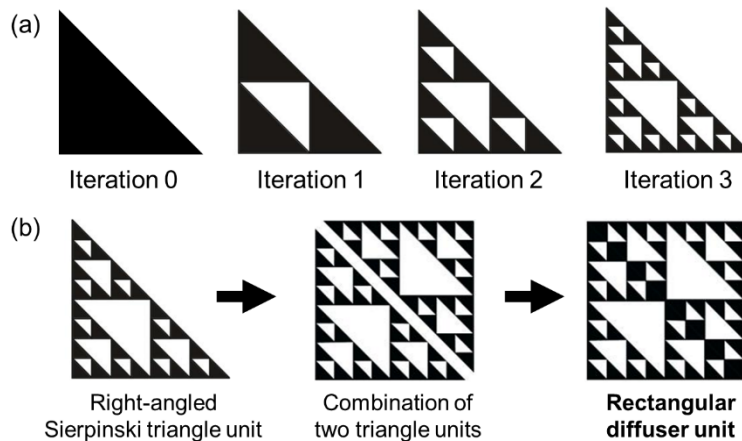
Fig. 1. Construction steps of (a) the Sierpinski triangle pattern and (b) the rectangular diffuser unit.
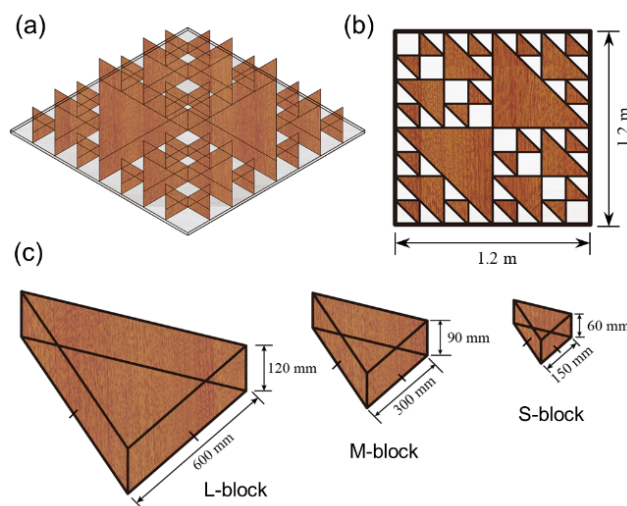

Fig. 2. (a) Isometric view and (b) top view of the Sierpinski-triangle diffuser.
(c) The dimensions of the large (L), medium (M), and small (S) blocks used.

The final design of the Sierpinski-triangle diffusers we propose in this work is made of triangular blocks of various sizes. Fig. 2(a) and 2(b) show the isometric and top view of the proposed design, respectively. All of the triangular blocks have flat tops, which are parallel to the bottom surfaces and to the diffusers' overall surfaces. The width and length of the diffusers are set to be 1.2 m × 1.2 m, considering the basic module size of the walls in the Chinese buildings (1.2 m), which have an advantage in the assembly and rearrangement according to the acoustic requirements of the space. The dimensions of the triangular blocks are shown in Fig. 2(c). The lengths of the one side of the triangle blocks are 600 mm, 300 mm, and 150 mm, and the heights of the blocks are 120 mm, 90 mm, and 60 mm for large (L), medium (M), and small (S) triangular blocks, respectively. Therefore, the overall size of the diffuser module becomes 1.2 m × 1.2 m × 120 mm.

Several parameters influence the diffusion performance of the proposed Sierpinski-triangle diffusers. To investigate these effects, case studies will be conducted by numerical simulations. The configurations of the scattering surfaces considered in the case studies are shown in Fig. 3. Firstly, we will investigate the influences of the number of iterations (group A). The modules are generated by iteration numbers 1, 2, 3, and 4, while the height of all triangle blocks is fixed as 60 mm. Smaller blocks than S-block in Fig. 2(c) are used in A4 case (iteration 4), and the size of the blocks is 75 mm × 75 mm × 60 mm. Secondly, for a chosen iteration number (iteration 3), the effect of the height of the blocks will be examined (group B). The height of the blocks will gradually increase from 30 mm to 120 mm with a 30 mm interval. Note that A3 and B2 are the same (iteration 3, height 60 mm). Based on the observations of the results from groups A and B, a Sierpinski-triangle diffuser with varying heights of blocks is presented (C1). Additionally, further modifications of C1 will be made by re-arranging triangular blocks and their performance will be compared with the diffuser based on the Sierpinski triangle (group C). By following terminologies used to represent the enclosed and semi-enclosed forms of buildings, C1-C4 are named as 'dispersed', 'semi-dispersed', 'semi-centralized', and 'centralized'. Note that the number of blocks used in C1-C4 is equal.

Group A	A1	A2	A3	A4
Iteration	1	2	3	4
Top view				
Front view				
Group B	B1	B2	B3	B4
Block height	30 mm	60 mm	90 mm	120 mm
Top view				
Front view				
Group C	C1	C2	C3	C4
Arrangement	Dispersed	Semi-dispersed	Semi-centralized	Centralized
Top view				
Front view				

Fig. 3. Configurations of scattering surfaces considered for case studies.

3. Numerical simulation

3.1 Simulation setup

Three-dimensional numerical simulations are conducted by using COMSOL Multiphysics 5.4®[31]. The BEM in Acoustic Module is used. As shown in Fig. 4, a scattering structure is surrounded by air (density ρ_0 = 1.21 kg/m^3, speed of sound c_0 = 343 m/s) and all boundaries of the structures are considered to be acoustically rigid. As mentioned in section 1, in this work, we focus on the evaluation of the diffusion performance in a near-field condition, and the far- field condition serves as a reference in Appendix C. The sound source is fixed 2.2 m above the center of the bottom surface of the diffuser and the receiver arc is placed 1.5 m above the scattering surface. According to the standardized measurement procedures mentioned in ISO 17497-2 [32], boundary plane measurements are used in numerical simulations. 35 receiver points are placed on the receiver arc, with an angular interval of 5°. The simulation domain is discretized with a maximum element size less than 1/10 of the minimum wavelength in the frequency range of interest. The numerical calculations are conducted at 4 frequencies per 1/3 octave band from 100 Hz to 5 kHz.
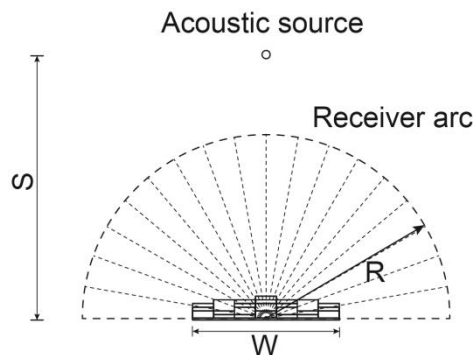

Fig. 4. Numerical simulation setup (S = 2.2m, R = 1.5 m, W = 1.2 m).

To evaluate the performance of the diffusers, acoustic diffusion coefficients are calculated by ISO 17497-2 [32]. For a fixed source position, the diffusion coefficient d_ψ can be calculated as

$$d_\Psi = \frac{\left(\sum_{i=1}^n 10^{L_i/10}\right)^2 - \sum_{i=1}^n \left(10^{L_i/10}\right)^2}{(n-1)\sum_{i=1}^n \left(10^{L_i/10}\right)^2},\qquad(1)$$

where L_i is sound pressure level (SPL) in decibels at i-th receiver position and n is the number of receivers. ψ denotes incidence angle. Only normal incidence is considered in this work, i.e., ψ = 0. Then, the normalized directional diffusion coefficient of the sample is calculated by

$$d_{\psi,n} = \frac{d_{\psi} - d_{\psi,r}}{1 - d_{\psi,r}}, \qquad\qquad (2)$$

where d_{ψ} and $d_{\psi,n}$ are the directional diffusion coefficients of the sample and the reference plane surface, respectively. The diffusion coefficients of the reference plane surface are presented in Appendix A. Once the normalized diffusion coefficients are calculated, the coefficients are averaged in 1/3 octave bands.

3.2 Simulation results

Fig. 5 shows the normalized diffusion coefficients $d_{0,n}$ of the diffusers of group A: the influence of the number of iterations. It is noticeable that all scattering surfaces in group A present the diffusion capacity starting from 315 Hz, i.e., the diffusion performances of the scattering surfaces are similar to or worse than that of the plane surface below 315 Hz. At 1 kHz, all the scattering surfaces have the highest diffusion coefficients. In the frequency bands from 315 Hz to 5 kHz, the performances of A1, A2, and A4 in frequencies above 1 kHz are generally worse than those in lower frequencies, especially above 2 kHz; the diffusion performances of fractal surfaces are similar to that of the plane surface, while A3 shows better diffusion performance in these frequency bands. The graph also shows that the overall diffusion coefficients increase as the number of iterations became larger for A1, A2, and A3, but A4 shows lower diffusion coefficients than A3, which suggests that there is an optimum number of iterations in the design of diffusers to have high performance. This can be explained by that the coverage area of the triangular blocks on the base panels increases as the number of iterations increases, i.e., the ratio of the coverage area is 25%, 44%, 57%, and 68% for A1-A4, sequentially. When the coverage area increases from 25% to 57%, the normalized diffusion coefficients varied from 0.24 to 0.52 at the frequency of 1 kHz, then the coefficients decrease in higher frequencies due to the lack of surface irregularities. In addition, the diffuser configuration has numerous wells formed in between the triangular blocks (areas colored in white in diffuser configurations) of which size decreases as the iteration number increases. The lateral size of the wells becomes comparable to the wavelength in the mid-high frequency range. This would cause the locally reacting behavior of the wells, which results in the waves being scattered in a specular direction.
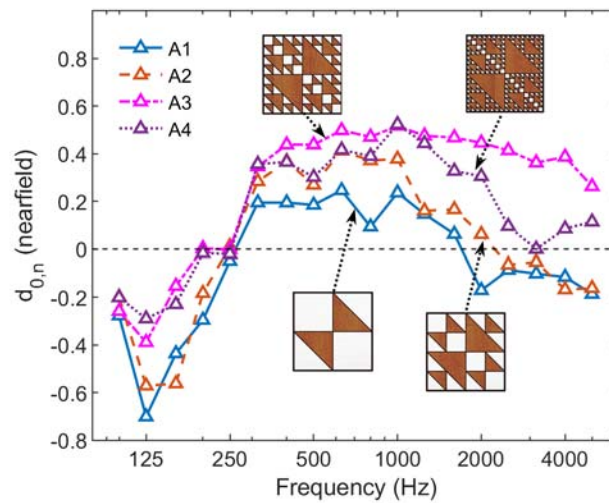
Fig. 5. Normalized diffusion coefficients of the diffusers in group A.

Fig. 6 shows the normalized diffusion coefficients $d_{0,n}$ of group B with four different heights 30 mm, 60 mm, 90 mm, and 120 mm. B1 features the lowest performance in the frequency range of interest compared with B2, B3, and B4. This is because the height of the blocks of B1 (30 mm) is much smaller compared to the wavelength of the sound waves, i.e., the wavelength of the highest frequency is around 85 mm in air, which is 2.57 times larger than the height of the blocks. When the wavelength is larger than a scattering obstacle, the waves are reflected in a specular direction rather than scattered in multiple directions and vice versa. Therefore, as the height increases, the diffusers in group B generally show enhanced diffusion performance. A similar trend to group A was found that all scattering surfaces in group B present better diffusion capacity compared with the reference plane surface in the frequency bands from 315 Hz to 5 kHz. As the height of the triangular blocks increases, the diffusion coefficients in mid-low frequency from 315 Hz to 1 kHz increase. However, it is also observable that in the frequency range above 1 kHz, the diffusion coefficients of the test samples of smaller heights are higher for B2-B4. In other words, the use of higher triangular blocks might increase the diffusion capacity of the diffuser in the low-frequency range, but the high-frequency performance is compromised. It is worth noting that the diffusion coefficient of B2 is higher than those of other types from 1.6 kHz to 5 kHz and has a small dip at 3.15 kHz, where the block height is a little greater than half of the wavelength of the sound waves in air at that frequency. This dip could be due to phase matching of the incident and reflected waves from the bottoms of blocks. In the cases of B3 and B4, decreasing trends are observed from 1.25 kHz, where the heights of the triangular blocks are close to half of the wavelength. Overall, the heights at 60 mm, 90 mm, and 120 mm for the Sierpinski-triangle diffuser give high values in the mid-high frequency range, thus combining those heights for this type of diffuser is a reasonable way to improve the diffusion performance in the mid-high frequency while keeping the low-frequency performance.

In Fig. 6, the normalized diffusion coefficients $d_{0,n}$ of C1, which is the diffuser with varying heights of blocks shown in Fig. 2, are presented along with the diffusion coefficients of diffusers of group B. The heights of the small, medium, and large triangle blocks are 60 mm, 90 mm, and 120 mm, respectively. C1 shows good diffusion capacity in the frequency range spanning from 250 Hz to 5 kHz, which is considered as being caused by the sequences generated between the structural heights of the blocks and the iteration patterns. To be specific, the diffusion performance of C1 in the mid-low frequencies below 500 Hz is comparable to that of B4. In the frequency range above 500 Hz, the diffusion performance of C1 is rather compromised compared to that of B2, B3, and B4, with a not very pronounced peak only at 1 kHz. This can be explained as that the heights of the triangular blocks are not consistent, the peaks related to the heights of the blocks do not appear anymore. However, it is noticeable that when a maximum height of 120 mm is considered (B4 and C1), C1 shows better performance in high frequencies (above 2 kHz) than B3 and B4. While the minimum height of 60 mm is compared (B2 and C1), C1 presents better performance in the mid-low frequencies (below 500 Hz) than B2. As an overall tendency, the effect of the combination of various heights of triangular blocks expands the effective frequency bands for the Sierpinski-triangle diffuser.
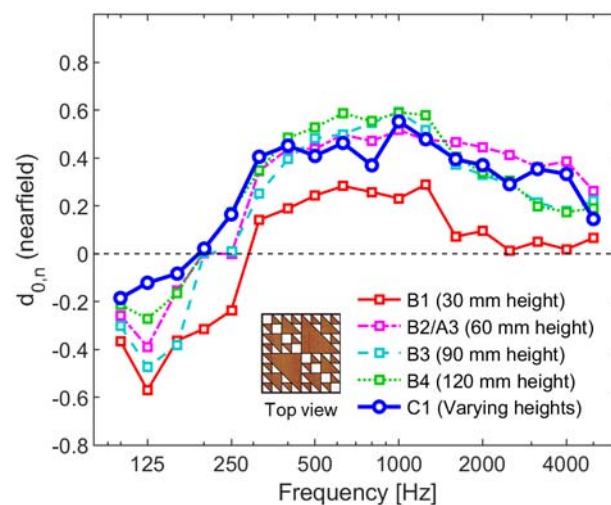

Fig. 6. Normalized diffusion coefficients of the diffusers in group B with four structural heights (h = 30 mm, 60 mm, 90 mm, and 120 mm). Normalized diffusion coefficients of C1 (with varying heights of blocks) are also presented for comparison.

Fig. 7 shows the normalized diffusion coefficients $d_{0,n}$ of the diffusers of group C. The purpose of this numerical experiment of group C is to confirm the effective diffusion capacity of the diffuser designed based on the fractal sequences over other structures, by changing the topology of the scattering surface. It is observable that when the blocks are more dispersed, the overall diffusion coefficients increase, i.e.,

type C1 (dispersed) has the highest diffusion coefficients followed by type C2 (semi-dispersed), C3 (semi-centralized), and C4 (centralized), sequentially. When C1 and C2 are compared, a decrease of normalized diffusion coefficients in the frequencies above 500 Hz is noticeable. When C2 and C3 are compared, the normalized diffusion coefficients in high frequencies are almost similar, however, C2 shows better diffusion performance in low frequencies than C3. On the other hand, C4 shows overall worse diffusion performance in the frequency range of interest. This is due to the different degrees in dispersion for the triangular blocks, resulting in varying amounts and widths of wells, and then the specular reflections formed in some area on the surfaces, which affect the scattering uniformity.

Fig. 7. Normalized diffusion coefficients of the diffusers in group C.

4. Experimental validation

4.1 Measurement setup

To validate the simulation results, diffusion coefficients obtained by measurements will be compared with the ones obtained by the simulation. The diffusers in group C are chosen for the experimental validation. Fig.8 shows photographs of the measurement samples. The test samples are made of pinewood boards and blocks. Triangular blocks are attached to the flat surface, which is a 15 mm-thick pinewood board of size 1.2 m × 1.2 m.
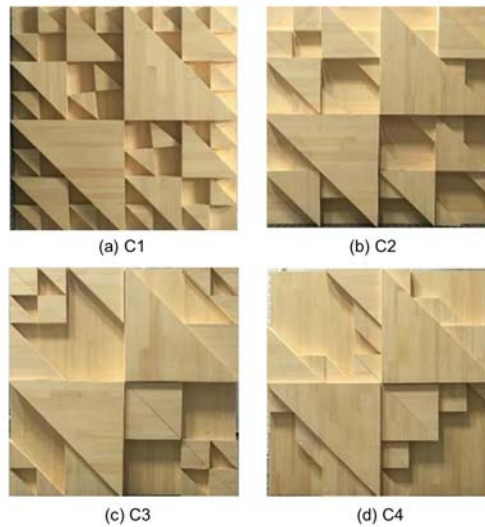
(a) C1   (b) C2

(c) C3   (d) C4

Fig. 8. Photographs of the measurement samples.

Fig. 9 shows the measurement setup. The measurements are conducted in the anechoic chamber of dimensions 12.1 m × 8.3 m × 7.9 m. The samples are placed on a test bench made of steel wire of dimension 3.0 m × 3.0 m × 0.3 m. Four corners contacting the suspended ground of the test bench are wrapped by polyurethane foam to suppress sound reflection by them. As same as in the simulation setting, a sound source is fixed 2.2 m above the center point of the reference flat surface. An impulse is generated by the sound source and the sound signals are captured by microphones. Microphones are placed on a semicircle of a radius of 1.5 m. According to the ISO 17497-2 [32], the test is suitably simplified compared to the simulation using a plane boundary. There are 17 receivers are placed at a maximum angular resolution of 10° on the receiver arc, instead of the 5°-resolution used in the simulation due to the limitation of the measurement setup. The microphones are moved by 10°, starting from 10° to 170°. The microphones are connected to a recording system (HEAD acoustics SQuadriga II). An audio analysis software (HEAD acoustics ArtemiS SUITE) is installed on a laptop to read the measured signals. After all data are collected, the diffusion coefficients are calculated by using Eq. (1).
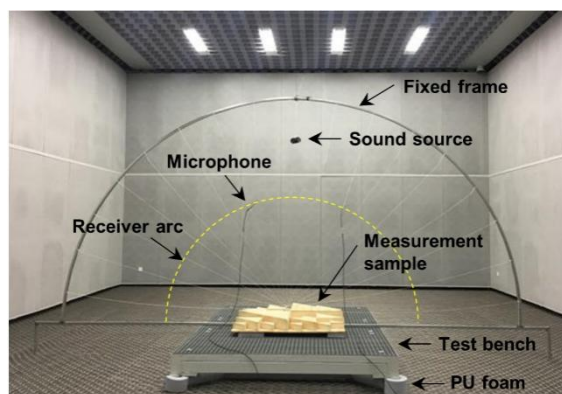

Fig. 9. Measurement setup. C1 diffuser is placed on the test bench.

4.2 Measurement results

Figs. 10 and 11 present the comparison of normalized diffusion coefficients under the normal incidence obtained by simulation and measurements. Fig. 12 shows the polar distribution of the scattered sound field under the normal incidence at 500 Hz, 1 kHz, 2 kHz, and 4 kHz for C1-C4, obtained by the numerical simulation and the measurements. Figs. 10 and 11 show that the measurement results show good agreement with the simulation results above 250 Hz, which confirms the validity of the simulation results presented in section 3. The discrepancies between the simulation and measurement results in the low frequencies (below 250 Hz) might be caused by the diffraction of the acoustic waves by the test bench. The diffusion performance of C1 is compared with that of a QRD with 2-dimensional gratings (N = 7) in Fig. 10, in order to show the advantage of the proposed Sierpinski-triangle diffuser over a conventional diffuser. The details of the QRD used in the comparison can be found in Appendix B. In the frequency above 1 kHz, the diffusion coefficients of C1 show a similar trend to that of the QRD. However, in frequency bands from 250 Hz to 1 kHz, C1 has higher diffusion coefficients than the QRD. The structural difference between the QRD and the proposed diffuser is that the proposed diffuser has relatively large blocks in lateral dimension compared to the blocks used in the QRD. It shows that the fractal patterns with various sizes of blocks have improved performance compared to the conventional QRD, especially in the mid-low frequency range.
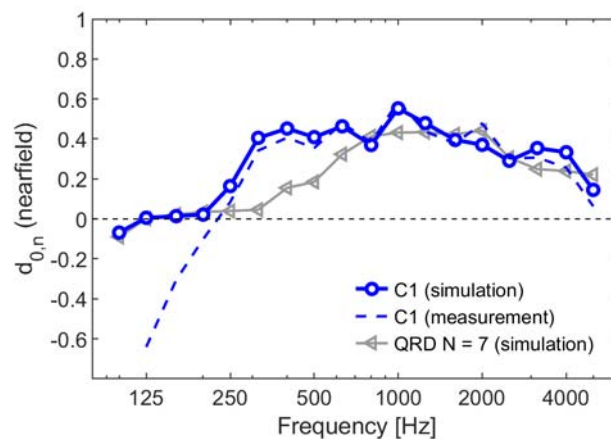

Fig. 10. Measured and simulated diffusion coefficients of C1 diffuser. Diffusion coefficients of QRD with 2-dimensional gratings (N = 7) are also compared.
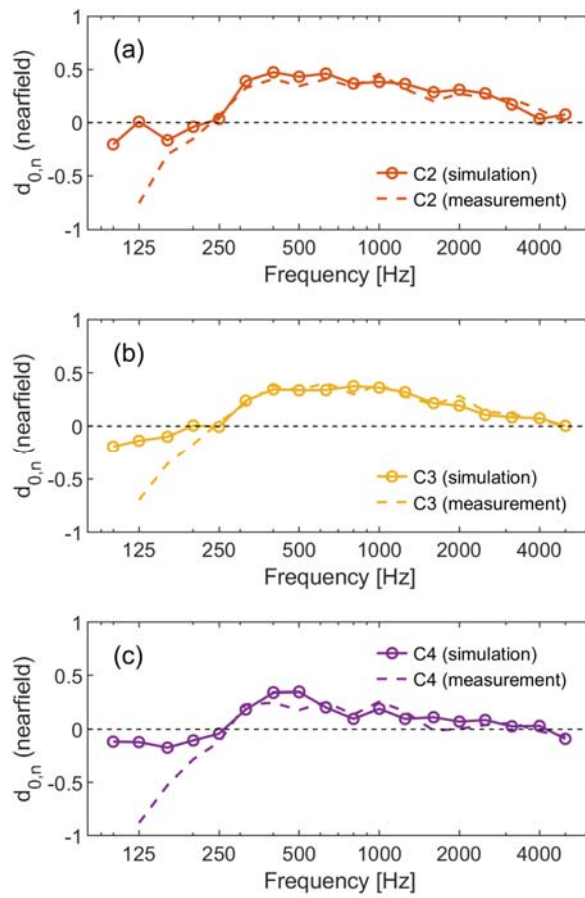
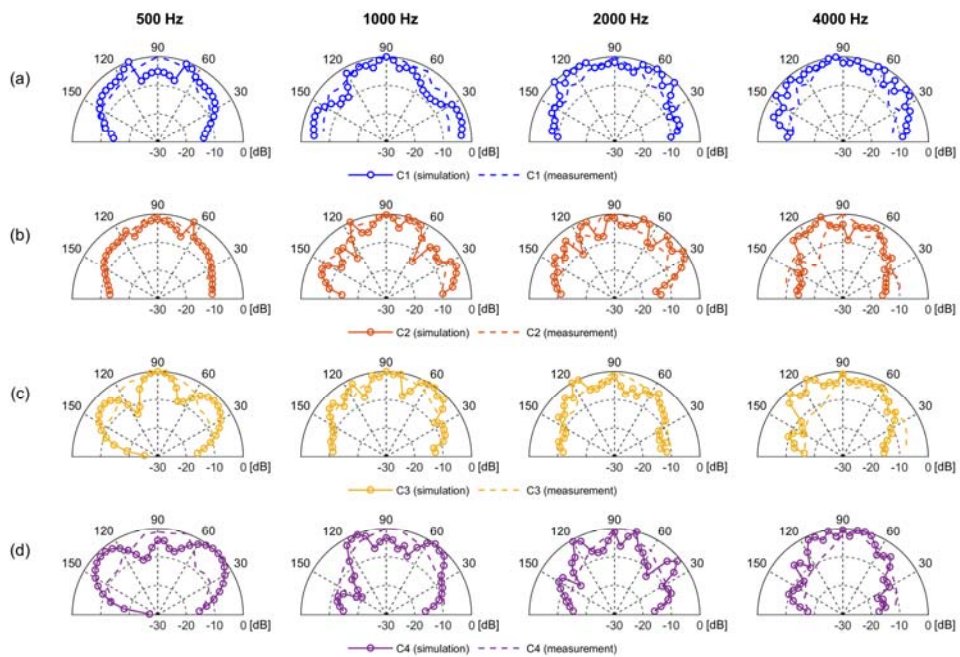**Fig. 11.** Measured and simulated diffusion coefficients of the diffusers in group C.

Fig. 12. Comparison of the simulation and measurement results of the scattered sound field by the diffusers (a) C1, (b) C2, (c) C3, and (d) C4 at 500 Hz,1 kHz, 2 kHz, and 4 kHz.

5. Conclusions

In this study, we demonstrated that the fractal acoustic diffusers showed improved acoustic diffusion capability in terms of bandwidth and low-frequency performance compared to the conventional QRD. The diffusers proposed in this study were designed based on the Sierpinski-triangle fractals which consist of a collection of various sizes of triangles. The Sierpinski-triangle diffusers were made of triangular blocks of various cross-sectional areas and heights.

Using 3D numerical simulations based on the BEM, we investigated the effects of the number of fractal iterations, the height of the triangular blocks, and arrangements of the blocks on the normal-incidence diffusion coefficients. The results showed that there is an optimum number of iterations (in this study, three) in the proposed diffusers to ensure high diffusion performance. Furthermore, it was demonstrated that as the height increases, the designed diffusers show enhanced diffusion performance in the low-frequency range, but the high-frequency performance is compromised. To improve the diffusion performance in the mid-high frequency while keeping the low-frequency performance, the diffusers combined with various heights of triangular blocks were presented. As a result, the combination of various heights of the triangular blocks expanded the effective frequency bands of the Sierpinski-triangle diffuser, and the diffusers showed the good diffusion capability in the frequency range spanning from 250 Hz to 5 kHz. In addition, other structures by changing the topology of the scattering surface were investigated. Consequently, when the blocks were more dispersed, the overall diffusion coefficients showed better performance.

The results of anechoic chamber measurements were presented to validate the numerical simulation results. The diffusive surfaces of different topologies were chosen for the experimental validation. The calculated diffusion coefficients as well as scattered polar responses were compared. The results obtained by the numerical simulations and the measurements showed excellent agreement, which confirmed the validity of the simulation results. Finally, we showed that the fractal patterns with various sizes of blocks improved diffusion performance compared to the conventional diffuser of the same size, especially in the mid-low frequency range.

The present work evaluated the diffuse performance of the Sierpinski-triangle diffusers under the normal-incidence condition. This is a pilot study and some preliminary results were obtained under limited conditions. Thus, in future works, it would be meaningful to investigate the diffusion performance under oblique- and random-incidence conditions. As the standards recommend, the measurement should be conducted under at least four directions of incidence, and the diffusion coefficients used to evaluate the diffusion properties should be averaged from the various incidence directions. Moreover, aiming to optimize the diffusion effect of the scattering surface, it would be meaningful to explore the influence of angled tops. Lastly, the enhancement of room acoustics by the Sierpinski-triangle diffusers in a real-sized room as well as the optimal combination pattern of the Sierpinski-triangle units can be investigated.

Acknowledgments

Appendix A. Diffusion coefficient of the plane surface

This appendix presents the diffusion coefficient of the flat reference panel in the near-field and far-field settings, which are used to normalize diffusion coefficients of the test samples in this work.
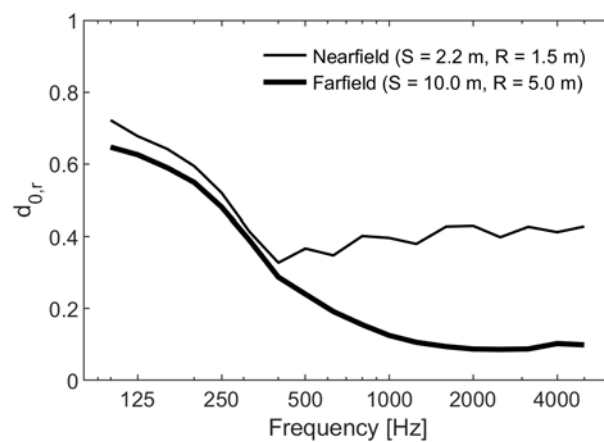

Fig. A1. Normal-incidence diffusion coefficients of the plane surface.

Appendix B. Quadratic residue diffuser (QRD)

This appendix presents the calculation method of the depths of the wells and configurations of the QRDs used for performance comparison in section 4.2. The QRDs consist of N wells where N is a prime number. A quadratic residue sequence is generated by

$$S_{n,m} = (n^2 + m^2) \bmod N , \tag{3}$$

where n and m are integers and index the sequence for the nth and m^{th} wells in the x and z directions, respectively, and *mod N* is the least non-negative remainder. Then the depth of n-th and m-th wells $d_{n,m}$ of is given as

$$d_{n,m} = S_{n,m} \frac{\lambda_0}{2N} , \tag{4}$$

where λ_0 is the wavelength of the design frequency. The design frequency of 830 Hz is used. The depths of the wells for two-dimensional QRDs are determined, where the heights of the blocks are approximately equal to the modules in the Sierpinski-triangle diffusers. The configurations of the QRDs with two-dimensional

gratings are presented in Figure B1. In this design, the width of each wells are the equal in the two directions and determined as 240 mm, 171.4 mm, and 92.3 mm for N = 5, 7, and 13, respectively.

Figure B2 shows the diffusion coefficients of QRDs presented in Figure B1, obtained by numerical simulations. It is observable that the diffusion coefficients of three types QRDs present similar trends, i.e., the diffusion coefficients increase as the frequency increases until they reach the maximum value at 1 kHz. After a small drop, the graphs have the second peaks at 2 kHz, and then generally decrease above 2 kHz. The performance of QRD (N = 13) and QRD (N = 7) is better than that of QRD (N = 5) in general, and QRD of N = 7 is presented in section 4.2 for the comparison of the performance with the Sierpinski-triangle diffuser.
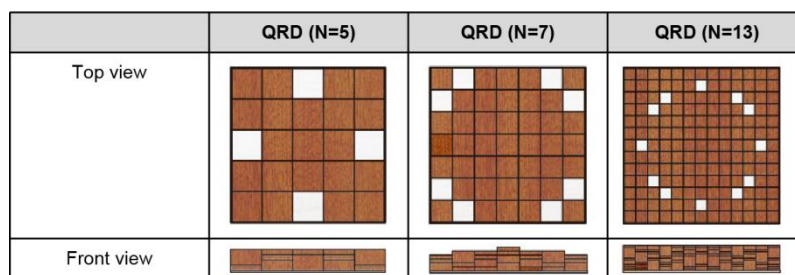

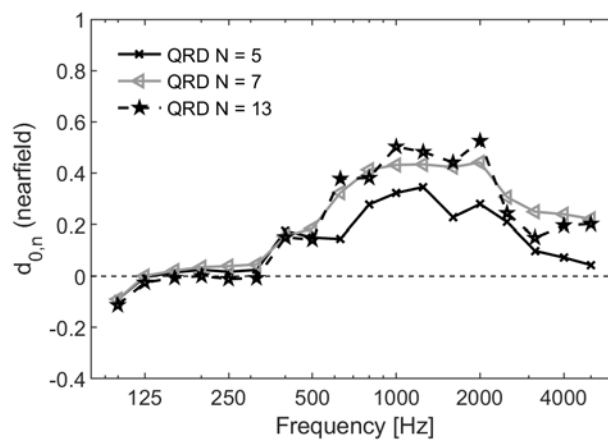**Fig. B1.** Configurations of the QRDs.

Fig. B2. Diffusion coefficients of the QRDs.

Appendix C. Simulation results in a far-field configuration

This appendix presents the numerical simulation results of test samples in the far-field using COMSOL Multiphysics 5.4® [31]. In the far-field simulations, the sound source is located 10 m above the bottom surface of the diffuser and the receiver arc is placed 5 m above the scattering surface, which follows the recommendation of ISO 17497-2 [32]that 80% of receivers are outside the specular zone. 35 receiver points are placed on the receiver arc, with an angular interval of 5°. Other simulation settings follow the description in section 3.1.

Figure C1, Figure C2, and Figure C3 show the normalized diffusion coefficients of the diffusers in groups A, B, and C, respectively. In general, all results in the far-field simulation show similar trends to the results obtained from the near-field configuration. In Fig. C3, the diffusion coefficients of the QRD (*N* = 7) are also presented for comparison. Again, it shows a similar trend with the near-field results that C1 presents better (below 2 kHz) or comparable (above 2 kHz) diffusion performance than QRD.
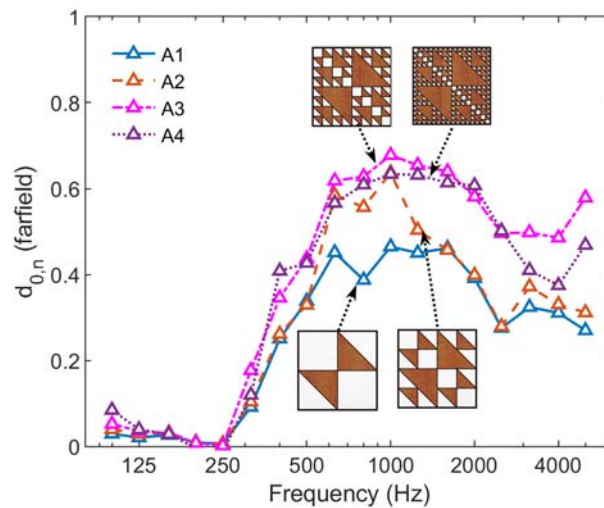

Fig. C1. Normalized diffusion coefficients of the diffusers in group A.
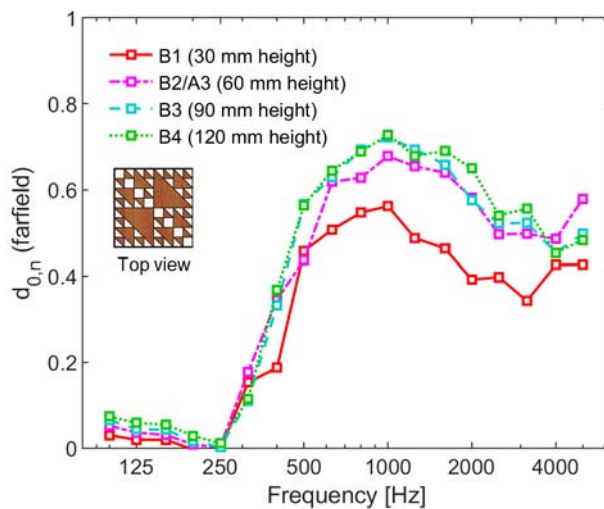

Fig. C2. Normalized diffusion coefficients of the diffusers in group B with four structural heights (*h* = 30 mm, 60 mm, 90 mm, and 120 mm).
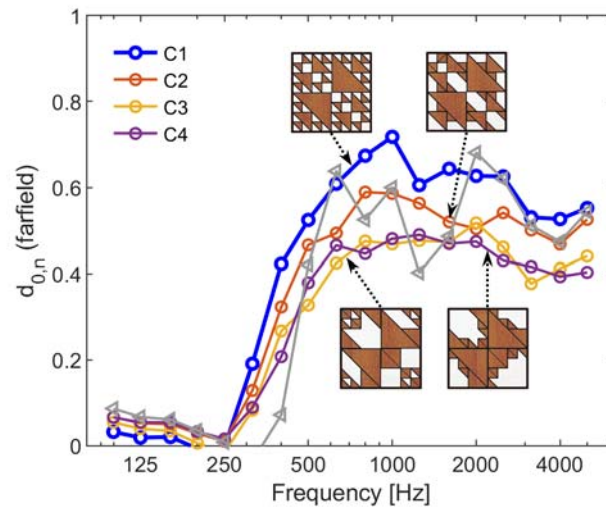
Fig. C3. Normalized diffusion coefficients of the diffusers in group C. Normalized diffusion coefficients of QRD with 2-dimensional gratings (N = 7, gray line) are also compared.

References

[1]Cox TJ, D'Antonio P. Acoustic absorbers and diffusers: theory, design and application. 3rd ed. Boca Raton, FL, USA: CRC Press; 2016.

[2]Jeon JY, Lee SC, Vorländer M. Development of scattering surfaces for concert halls. Appl Acoust 2004;65:341–55. https://doi.org/10.1016/j.apacoust.2003.11.001.

[3]Kang J. Experimental approach to the effect of diffusers on the sound attenuatioin long enclosures. Building Acoustics 1995;2(1):391–402. https://doi.org/10.1177/1351010X9500200105.

[4]Kim YH, Jang HS, Jeon JY. Characterizing diffusive surfaces using scattering and diffusion coefficients. Appl Acoust 2011;72:899–905. https://doi.org/10.1016/ j.apacoust.2011.05.006.

[5]Tsuchiya Y, Lee H, Sakuma T. Scale model measurement of the scattering coefficients of rib/block structure walls. Archit Inst Jpn J Technol Des 2013;19:175–8. https://doi.org/10.3130/aijt.19.175.

[6]Choi Y-J. Effects of periodic type diffusers on classroom acoustics. Appl Acoust 2013;74:694–707. https://doi.org/10.1016/j.apacoust.2012.11.010.

[7]Cox TJ. Designing curved diffusers for performance spaces. J Audio Eng Soc 1996;44:354. http://www.aes.org/e-lib/browse.cfm?elib=7901.

[8]D'Antonio P, Cox TJ. Aperiodic tiling of diffusers using a single asymmetric base shape, Proceedings of the 18th ICA, Kyoto,2004;paper Mo2.B2.3.

[9]Shtrepi L, Mendéz Echenagucia T, Badino E, et al. A performance-based optimization approach for diffusive surface topology design. Build Acoust 2020; 28:231–47. https://doi.org/10.1177/1351010X20967821.

[10]Yang H-S, Kang J, Cheal C. Random-incidence absorption and scattering coefficients of vegetation. Acta Acustica united with Acustica 2013;99 (3):379–88. https://doi.org/10.3813/AAA.918619.

[11]Peters B, Olesen T. Integrating Sound Scattering Measurements in the Design of Complex Architectural Surfaces:Informing a parametric design strategy with acoustic measurements from rapid prototype scale models. India, Australia: ETH Zurich; 2010. p. 481–91.

[12]Shtrepi L, Menichelli J, Astolfi A, et al. Improving scattering surface design with rapid feedback by integrating parametric models and acoustic simulation.J Acoust Soc 2017;142:2499. https://doi.org/10.1121/1.5014125.

[13]Reinhardt D, Cabrera D, Jung A, et al. Towards a micro design of acoustic surfaces. In: Robotic fabrication in architecture, art and design. Cham:Springer International Publishing, 2016;137-151.10.1007/978-3-319-26378-6.

[14]Schroeder MR. Diffuse sound reflection by maximum-length sequences. J Acoust Soc 1975;57:149–50. https://doi.org/10.1121/1.380425.

[15]Schroeder MR. Binaural dissimilarity and optimum ceilings for concert halls: more lateral sound diffusion. J Acoust Soc 1979;65:958–63. https://doi.org/ 10.1121/1.382601.

[16]De Jong BA, Van Den Berg PM. Theoretical design of optimum planar sound diffusers. J Acoust Soc 1980;68:1154. https://doi.org/10.1121/1.385000.

[17]Herrero JM, Blasco X, Sanchez-Perez JV, et al. Design of sound phase diffusers by means of mutiobjective optimization approach using ev-MOGA evolutionary algoritum. Struct Multidsc Optim 2016;53:861–79.https://doi. org/10.1007/s00158-015-1367-0.

[18]Cox TJ. The optimization of profiled diffusers. J Acoust Soc Am 1995; 97:2928–36. https://doi.org/10.1121/1.412972.

[19]Angus JAS. Using grating modulation to achieve wideband large area diffusers. Appl Acoust 2000;60:143–65. https://doi.org/10.1016/S0003-682X(99)00047- X.

[20]Zhu Y, Fan X, Liang B, et al. Ultrathin acoustic metasurface-based schroeder diffuser. Phys Rev X 2017;7.https://doi.org/10.1103/ PhysRevX.7.021034021034.

[21]Jiménez J, Cox TJ, Romero-García V, et al. Metadiffusers: Deep-subwavelength sound diffusers. Sci Rep 2017;7(1):1–12. https://doi.org/10.1038/s41598-017- 05710-5.

[22]Cox TJ. Acoustic diffusers: the good, the bad and the ugly. Proceedings of the Institute of Acoustics. The Salford University.

[23]Le CTP. Fractal geometry and applicability to biological simulation shapes for sustainable architecture design in Vietnam. Environ Sci Pollut Res 2021;28:12000–10. https://doi.org/10.1007/s11356-020-08417-9.

[24]Cox TJ. Fractal sound diffusers. Great Britain. J Audio En g Soc 1997;45:1020.

[25]Lee H, Tsuchiya Y, Sakuma T. Acoustic scattering characteristics of Penrose- tiling-type diffusers. Appl Acoust 2018;130:168–76. https://doi.org/10.1016/j. apacoust.2017.08.022.

[26]Bradley, David, et al. Numerical prediction of sound scattering from surfaces with fractal geometry: A preliminary investigation. Proceedings of Meetings on Acoustics 161ASA. Vol. 12. No. 1. Acoustical Society of America, 2011.10. 1121/1.4862555.

[27]Olson, Derek R., David T. Bradley. Fractal surfaces: Generation and acoustic scattering prediction.J Acoust Soc 2009; 125.4: 2613-2613. 10.1121/ 1.4783953.

[28]Perry T, Dr Driessen P. The lean optimization of acoustic diffusers: design by artificial evolution, time domain simulation and fractals. University of Victoria-Faculty of Engineering; 2011.

[29]Rasouli Kenari A, Solaimani M. Optical properties of two dimensional fractal shaped nanostructures: Comparison of Sierpinski triangles and Sierpinski carpet.OptCommun 2020; 474. https://doi.org/10.1016/j. optcom.2020.126185.

[30]Xu H, Ni F, Wu J. Multi-level modular wooden diffusers based on fractal theory. 2018 World Conference on Timber Engineering (WCTE), Seoul, 20–23 August 2018.

[31]COMSOL Multiphysics® v. 5.4. COMSOL AB, Stockholm, Sweden.

[32]ISO 17497-2. Acoustics-Sound-scattering properties of surfaces. Part 2: Measurement of the directional diffusion coefficient in a free field, Geneve; 2012.